

Construction of A Double-Walled Carbon Nanoring

Chong Zhao, Fupin Liu, Lai Feng, Mingzhe Nie, Yuxi Lu, Jie Zhang, Chunru Wang, and Taishan Wang*

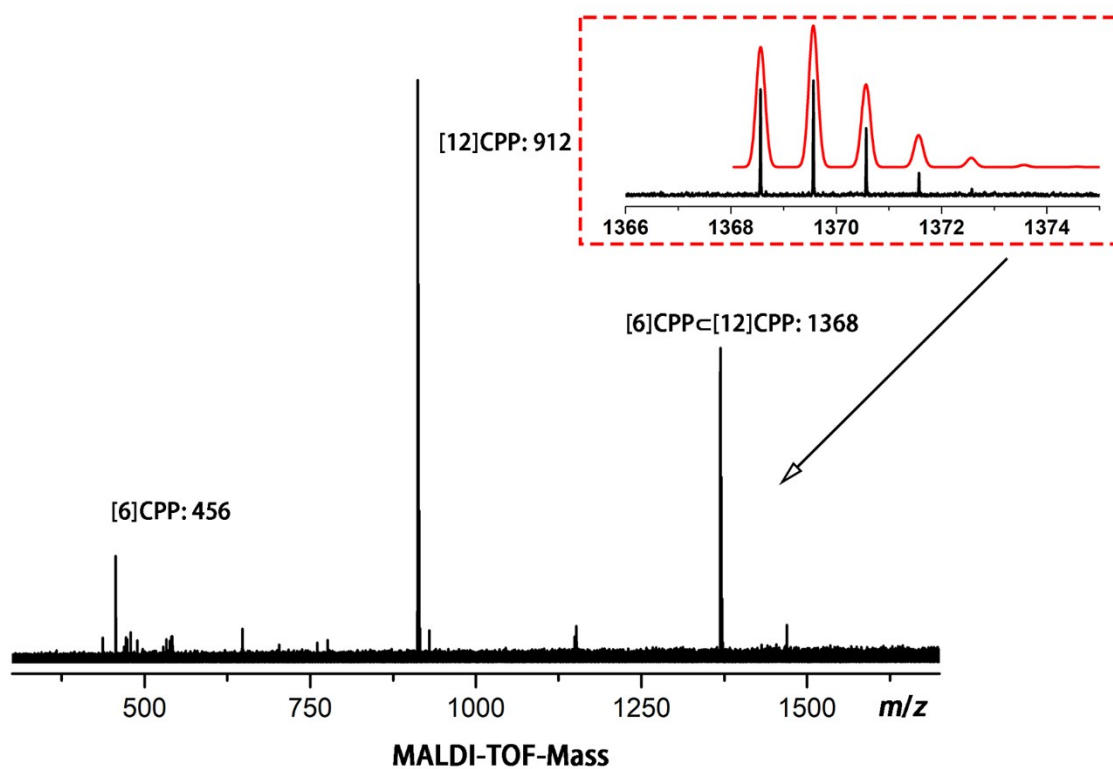


Figure S1. High resolution MALDI-TOF mass spectrum of [6]CPP<[12]CPP.

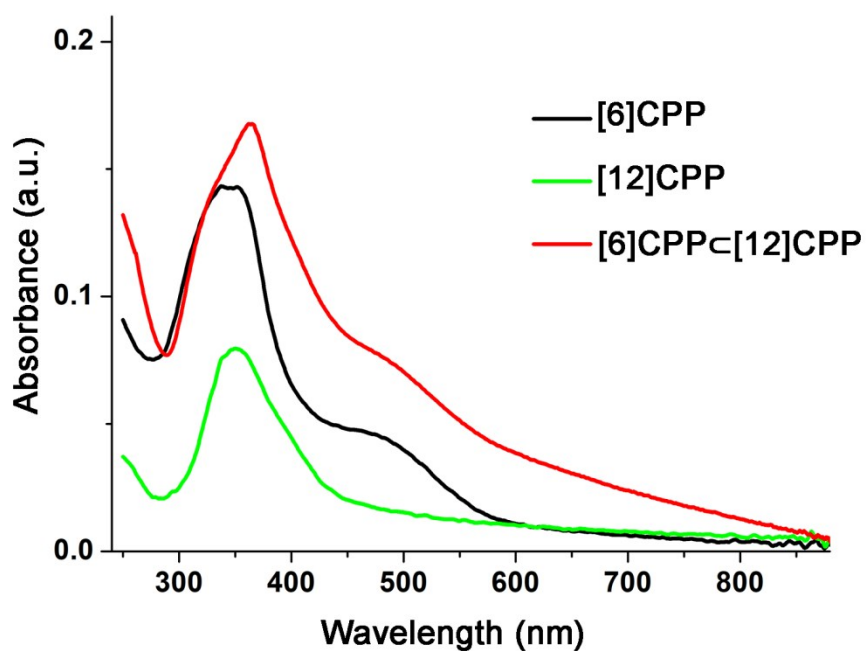


Figure S2. UV-Vis spectra of [6]CPP, [12]CPP, and [6]CPP<[12]CPP films. The thin film was spin-coated (60 μ L) on the quartz glass substrate using the samples with the same concentration of 1.0×10^{-3} mol/L in CH_2Cl_2 .

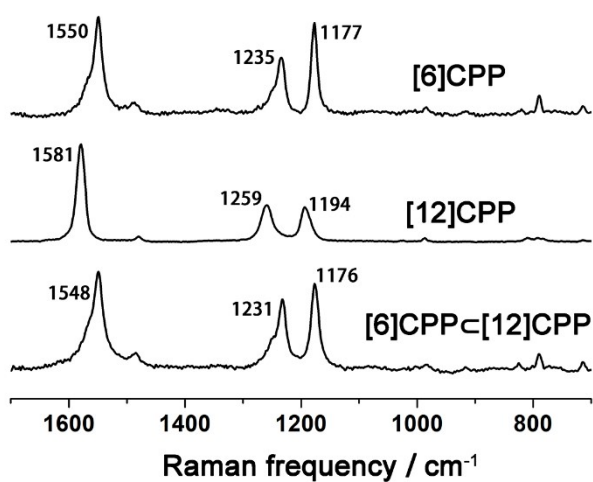


Figure S3. Raman spectra of [6]CPP, [12]CPP, and [6]CPP<[12]CPP in solid state.

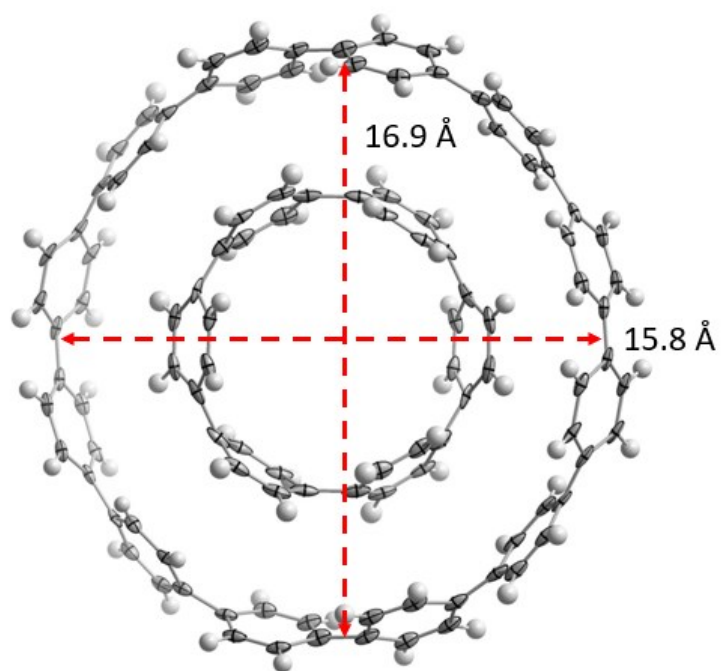


Figure S4. The long and short axes of the ellipse [6]CPP/[12]CPP crystalline structure.

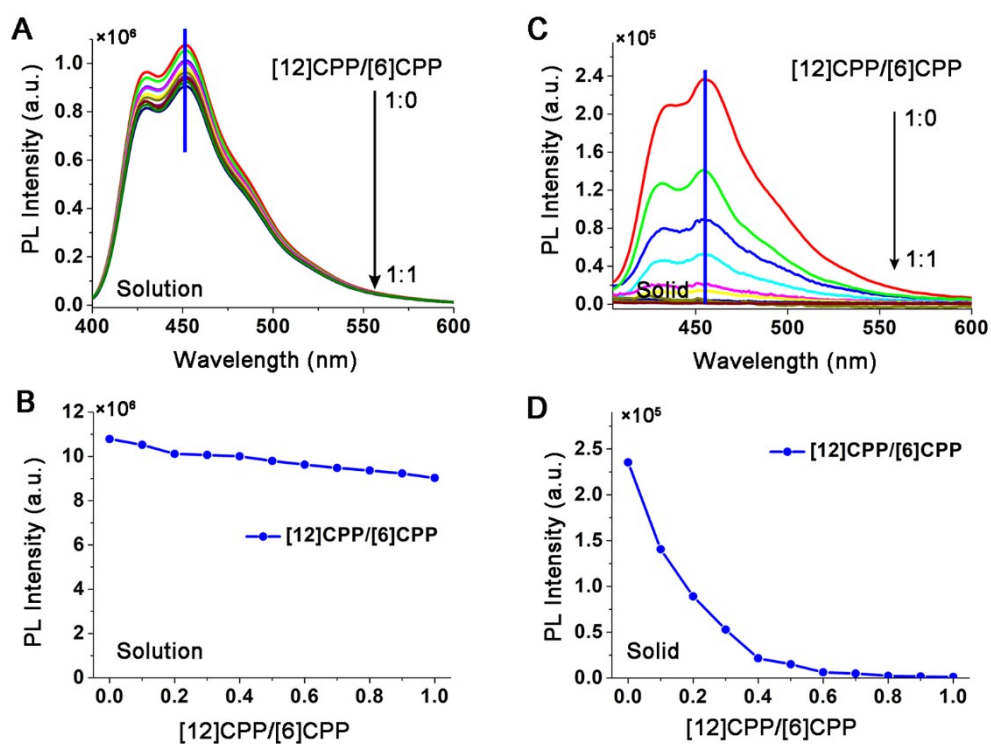


Figure S5. Fluorescence titrations of [12]CPP with increasing amounts of [6]CPP in CH₂Cl₂ solution and solid states following titration experiments. (a) Solution state titration and (b) the job plot of [12]CPP (1.5 M) with 0 ~ 1.5 M [6]CPP. (c) Solid state titration and (d) the job plot of [12]CPP (1.5 M) with 0 ~ 1.5 M [6]CPP. The λ_{exc} is 385 nm, and the job plots were monitored at 460 nm.

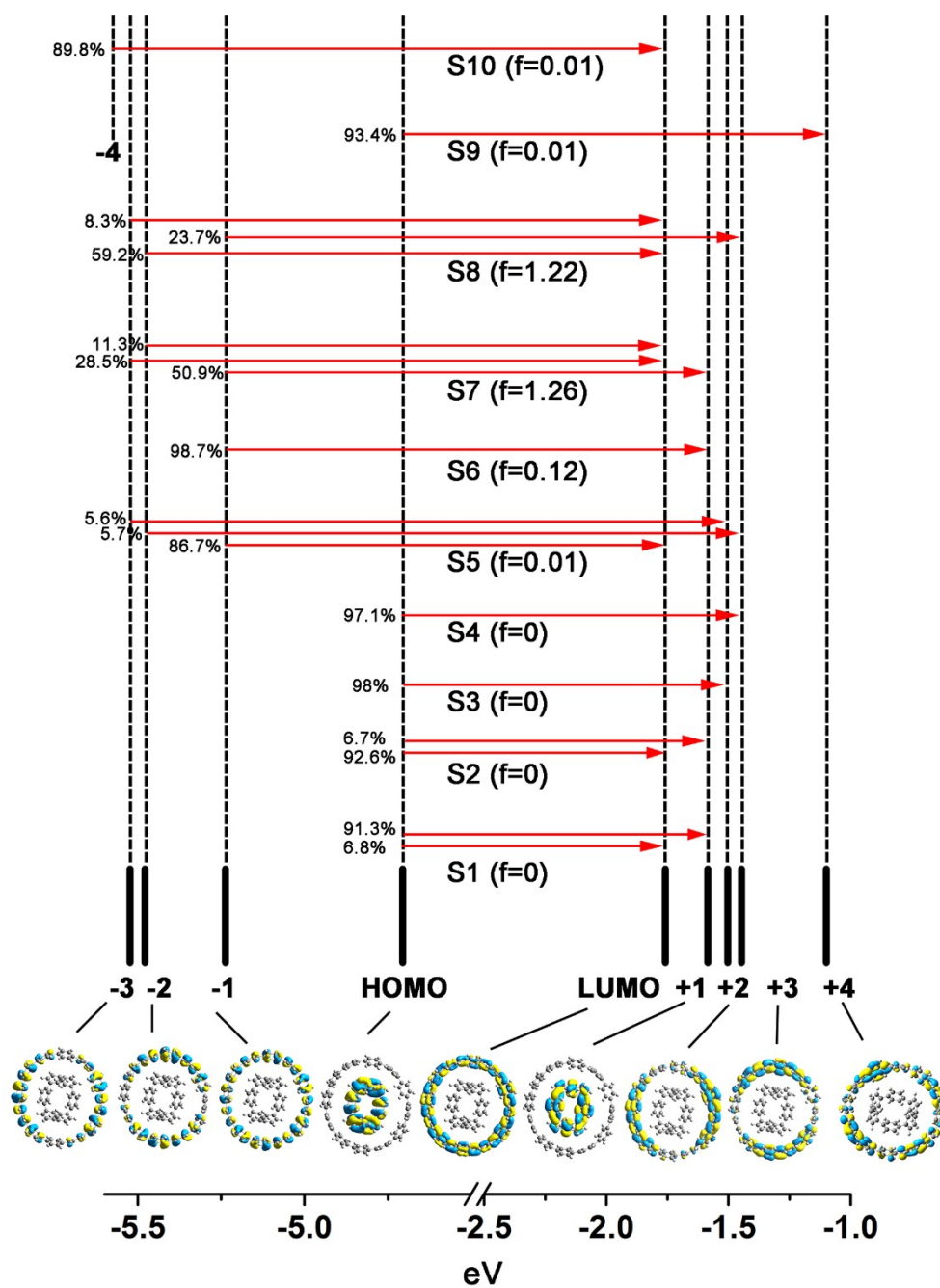


Figure S6. MOs and orbital visualizations of the calculated front 10 vertical excited states.

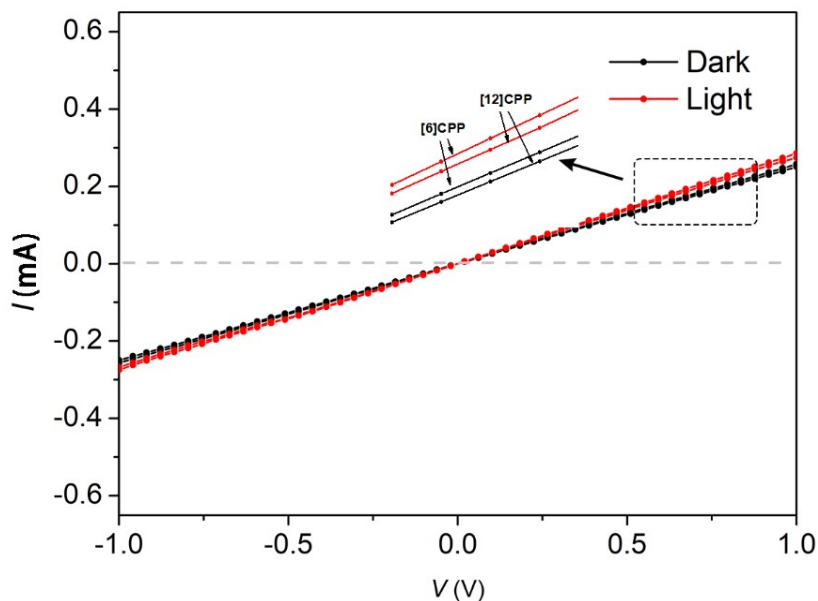


Figure S7. I - V profiles of the [6]CPP and [12]CPP with (red) and without (black) photoirradiation.

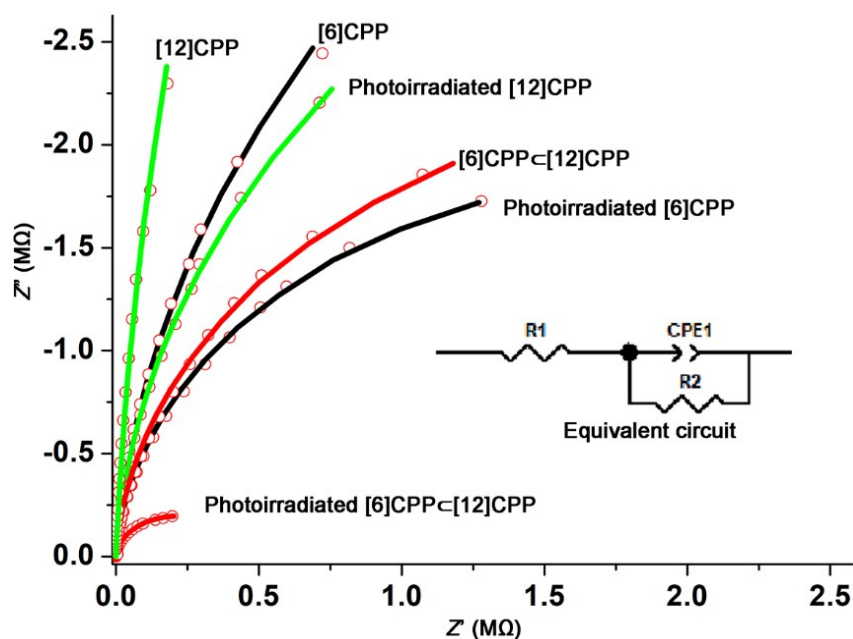


Figure S8. Nyquist plots before and after the photoirradiation applied to [6]CPP (black), [12]CPP (green), and [6]CPP/[12]CPP (red) films. Inset is the simulated equivalent circuit.

Table S1. Simulated impedance results for the plots before and after the photoirradiation. Unit, $\Omega \text{ cm}^2$.

	[12]CPP	[6]CPP	[6]CPP<[12]CPP
Dark	5.75×10^7	1.18×10^7	4.65×10^6
Photoirradiation	8.78×10^6	3.87×10^6	4.24×10^5

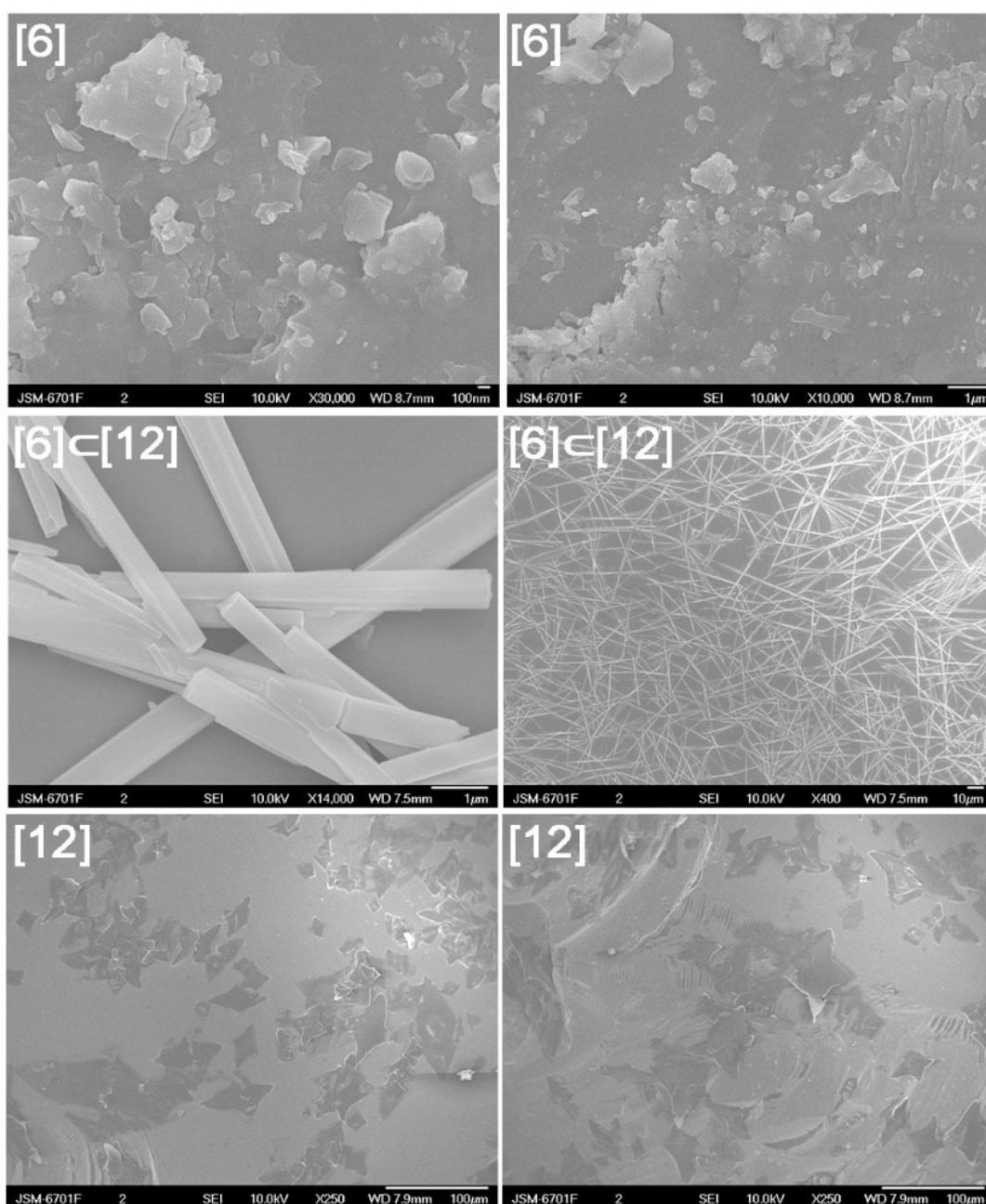


Figure S9. SEM images of [6]CPPs, [12]CPP, and [6]CPPs<[12]CPP complexes in DMF solution.

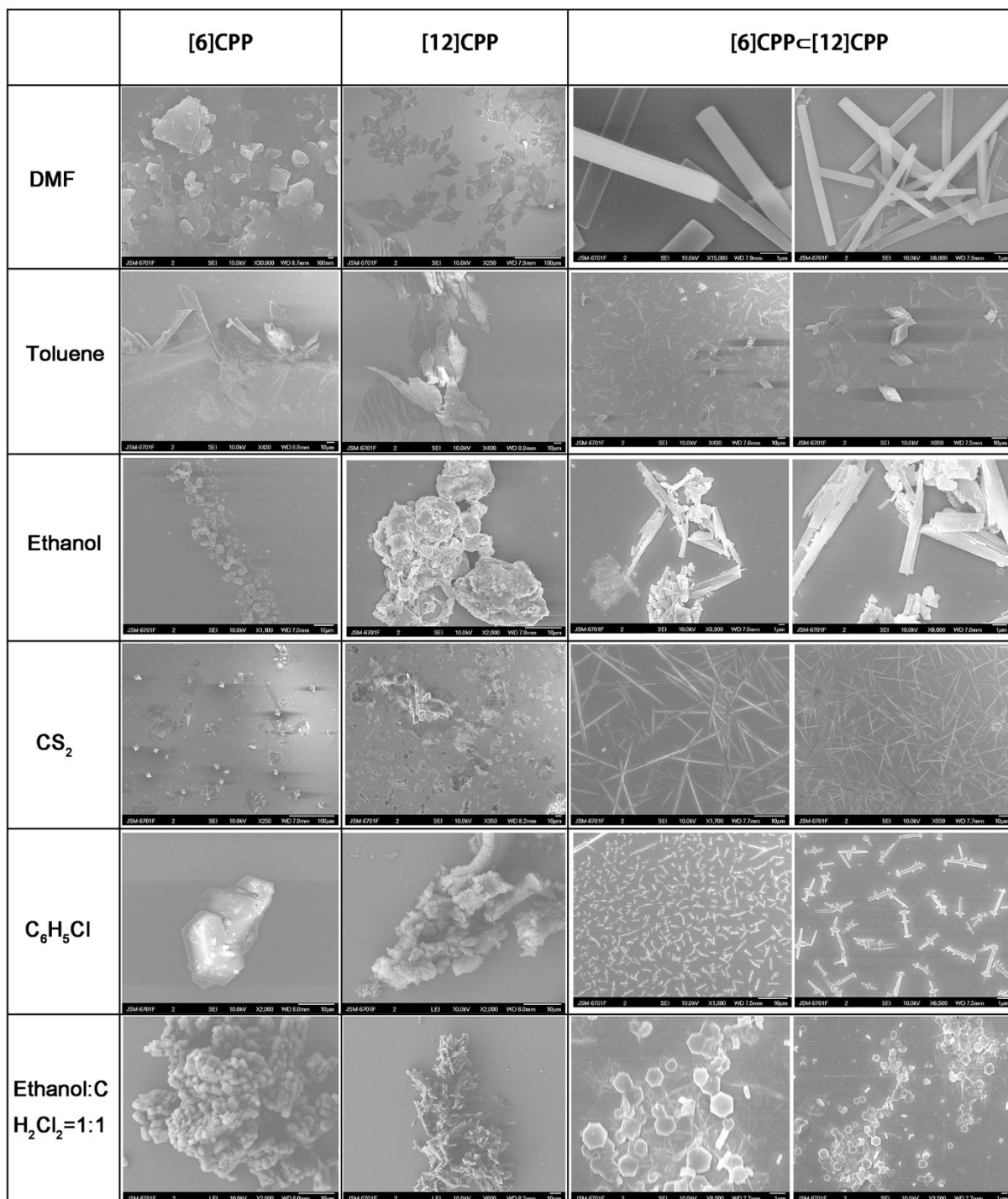


Figure S10. SEM images of [6]<[12]CPP complex in different solutions.

Structures_[6]CPP<[12]CPP

X-ray diffraction data collection was carried out using a diffractometer (Rigaku Saturn724+) equipped with a CCD collector. The structure was solved by direct methods and refined by SHELXL-2018.^[1] Hydrogen atoms were added geometrically, and refined with a riding model. The crystal data are presented in Table S2.

Figure 2a presents the packing of the [6]CPP⊂[12]CPP molecules in the crystal lattice, the dichloromethane molecules are located in the voids of the [12]CPP molecules, the severely disordered solvent molecules are observed to locate in the center of the [6]CPP molecules, which is masked with SQUEEZE code in the refinement.^[2] The angle between [6]CPP and [12]CPP evaluated with dihedral angle of the least squares planes pass through the [6]CPP/[12]CPP is 26.7(5)°.

Table S2. Crystal data _[6]CPP⊂[12]CPP.

Crystal	6CPP⊂12CPP
Formula	C ₅₅ H ₃₈ Cl ₂
Formula weight	769.75
Color, habit	yellow, block
Crystal system	monoclinic
Space group	P2 ₁ /c
<i>a</i> , Å	6.2639(6)
<i>b</i> , Å	22.294(2)
<i>c</i> , Å	30.280(4)
<i>α</i> , deg	90
<i>β</i> , deg	95.509(10)
<i>γ</i> , deg	90
Volume, Å³	4209.0(8)
<i>Z</i>	4
<i>T</i>, K	170
Radiation (λ, Å)	Mo K-α (0.71073)
Unique data (<i>R</i>_{int})	9593 (0.2142)
Parameters	515

Restraints	366
Observed data ($I > 2\sigma(I)$)	2971
R_I^a (observed data)	0.1876
wR_2^b (all data)	0.4620
CCDC NO.	2013130

^aFor data with $I > 2\sigma(I)$, $R_1 = \frac{\sum ||F_o| - |F_c||}{\sum |F_o|}$. ^bFor all data, $wR_2 = \sqrt{\frac{\sum [w(F_o^2 - F_c^2)^2]}{\sum [w(F_o^2)^2]}}$.

Reference:

- [1] G. Sheldrick, *Acta Cryst. C* **2015**, 71, 3.
- [2] A. Spek, *Acta Cryst. C* **2015**, 71, 9.